Disorder-Oriented Genetic Algorithm for Exploration Optimisation in Robot Swarms

Gabriel A. C. Batista[1], **Eduardo S. Rocha**[1], **Claudiney R. Tinoco**[1]

[1]Department of Computing, Federal University of Uberlândia
2121, João Naves de Ávila Ave., 38.408-100, Uberlândia, MG, Brazil

{gabriel.alcantara, eduardo.rocha, claudiney.tinoco}@ufu.br

Abstract. *Parameter selection is a critical aspect of robot swarm coordination, as it directly affects collective behaviour and task performance. However, manually determining these parameters becomes increasingly difficult as environmental complexity and task requirements increase. In this context, this work proposes the application and adaptation of an evolutionary algorithm to optimize the parameters of the PheroCom model for swarm coordination. To achieve this, entropy is incorporated as an evaluation metric in the fitness function, acting as a multiplicative factor within a penalty scheme during task execution. This allows the identification of parameter settings that promote a more balanced spatial distribution of robots, improving environmental coverage while avoiding both excessive concentration and neglected regions. Experimental results show that incorporating entropy into the evaluation criterion provides an effective measure of exploration uniformity and leads to a more consistent distribution of robots throughout the environment. In addition, the optimized model achieves competitive performance compared with the reference configuration.*
Keywords: *Swarm Robotics. Genetic Algorithms. Parameter Optimization. Entropy. Environment Coverage. Bio-inspired Algorithms.*

1. Introduction

Robotics has advanced rapidly in recent years, leading to the development of increasingly sophisticated solutions for real-world problems [Raj and Kos 2022]. As robotic applications become more complex and data-intensive, greater attention must be given to the design of efficient control and coordination mechanisms. This challenge is particularly evident in swarm robotics and bio-inspired systems [Shahzad et al. 2023], where collective behaviour emerges from local interactions among multiple robots. In such scenarios, small changes in parameter settings may result in significantly different swarm behaviours, making parameter tuning a non-trivial task.

Robot swarms have emerged as an alternative to centralized and hierarchical control systems by promoting distributed decision-making and cooperation among autonomous agents. According to [Şahin 2004], scalability, robustness, and flexibility are fundamental properties that enable swarm systems to operate under uncertainty, adapt to dynamic environmental changes, and remain functional despite individual failures. These characteristics have motivated the application of swarm robotics in several practical domains, including collaborative space exploration [Huang et al. 2020] and infrastructure inspection [Halder and Afsari 2023].

In this context, defining suitable coordination strategies and parameter configurations becomes essential to ensure efficient task execution. However, the stochastic nature of swarm systems often makes manual parameter tuning difficult and time-consuming. As a result, evolutionary optimization techniques have attracted increasing attention in the literature [Zhan et al. 2022]. Among them, Genetic Algorithms (GA) provide an effective mechanism for exploring large search spaces through evolutionary operators inspired by natural selection [Papazoglou and Biskas 2023], making them particularly suitable for parameter optimization in swarm coordination models.

Given this scenario, this work investigates the use of GAs to optimize the parameters of the PheroCom model [Tinoco et al. 2025] for swarm coordination. To guide the evolutionary process, the fitness function incorporates entropy-based measures that evaluate the spatial distribution of robots during the surveillance task. The proposed approach seeks to identify parameter configurations that promote more homogeneous environmental coverage while maintaining high collective performance.

This work is organized as follows: (i) Section 2 presents the theoretical background and discusses related works, the PheroCom model, a brief description of entropy, and the Task-Points metric; (ii) Section 3 introduces the proposed approach for parameter optimisation; (iii) Section 4 details the experiments carried out and discusses the results; finally, (iv) Section 5 presents the main conclusions and future works.

2. Theoretical Framework

This section reviews the related work on exploration with robot swarms, describes the PheroCom model, and defines entropy and task-points.

2.1. Related Works

Recent studies have explored GAs for optimization in robotics, including path planning and multi-robot coordination. In path planning, [Cheng et al. 2020] proposed a multi-objective GA for reconfigurable robots, while [Hao et al. 2020] introduced a multipopulation migration-based approach to improve population diversity and reduce premature convergence. For multi-robot formation, [López-González et al. 2020] employed a parallel GA to optimize distances, angles, and velocities between robots, while [Ma et al. 2020] used genetic operators to generate smooth and safe Bézier-based trajectories.

Evolutionary approaches have also been applied to collective robotic systems and parameter optimization. [Stolfi et al. 2020] proposed a cooperative coevolutionary approach for optimizing a pheromone-based coverage model in UAV swarms. More directly related to this work, [Tinoco et al. 2020] employed GAs to optimize the IACA-DI swarm coordination model, demonstrating improvements over empirical parameter tuning. [Nonoyama et al. 2022] used metaheuristic algorithms to optimize PID parameters for industrial robot energy efficiency, while [Torres et al. 2024] investigated GAs for dynamic route optimization in mobile robots.

As summarized in Table 1, existing studies mainly focus on navigation, control, and parameter optimization. However, few explicitly address homogeneous spatial distributions in swarm surveillance tasks. To fill this gap, this work incorporates entropy into the fitness evaluation process, enabling the identification of parameter configurations that promote more uniform coverage while maintaining collective performance.

Table 1. Comparison of GA applications, robotics, and parameter optimization.

Authors	Optimization	Robots [multi-robot]	Genetic Algorithms	
			Generations	Initial Pop.
[Cheng et al. 2020]	✓	Yes [no]	25;50;100	1000
[Hao et al. 2020]	×	Yes [no]	200;500	60;120
[López-González et al. 2020]	×	Yes [yes]	1000	1000
[Ma et al. 2020]	✓	Yes [no]	50;100	100
[Stolfi et al. 2020]	✓	Yes [yes]	—	—
[Tinoco et al. 2020]	✓	Yes [yes]	100	100
[Nonoyama et al. 2022]	✓	Yes [no]	10;20;30;50	100;200;300;
[Torres et al. 2024]	✓	Yes [no]	100	50
This work	✓	**Yes [yes]**	**100**	**50;100;150**

2.2. PheroCom Model

The PheroCom, proposed by Tinoco and Oliveira [Tinoco et al. 2025], is a framework that virtualises and controls pheromone dynamics to coordinate robot swarms. Each robot follows a Finite State Machine (FSM) (Fig. 1), which governs local decision-making through predefined rules during task execution and information exchange.

Robots store pheromone data locally, using a repulsive pheromone effect to discourage unnecessary revisits, promote dispersion, and prevent clustering. The model operates without a central controller, with robots exchanging local pheromone data with nearby peers. This mechanism is inspired by ant vibroacoustic communication and enables information propagation across the swarm.

Although each robot makes decisions based on local information, the interaction among robots produces the desired global behaviour. Furthermore, running the same FSM across the swarm preserves decentralisation and allows the task to continue even when part of the swarm fails, providing robustness against individual robot failures.

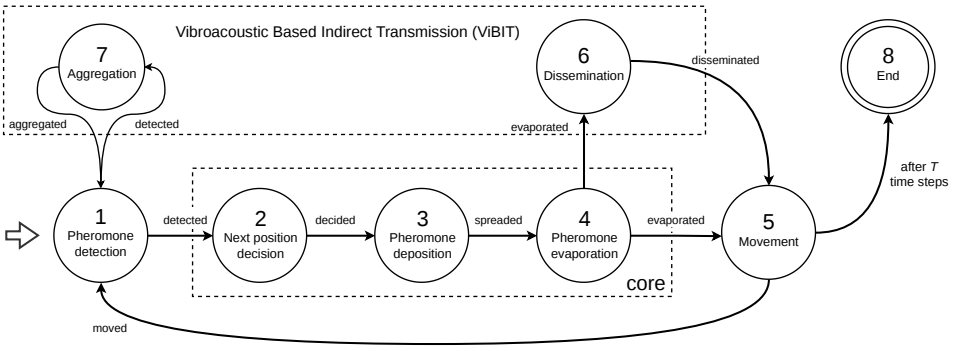


Figure 1. Individual robot behaviour FSM [Extracted from [Tinoco et al. 2025]].

FSM states 1 to 5 form the main cycle and use pheromone data to guide decisions. States 6 and 7 handle inter-robot communication, while state 8 marks termination. Each cycle corresponds to one asynchronous time-step. The environment is represented by two grids: a physical grid for obstacles, free space, and neighbours; and a pheromone grid containing pheromone concentrations. All FSM states rely on data from these grids.

According to [Tinoco et al. 2025], the states of the FSM are as follows:

- *State 1 - Pheromone Detection*: the robots detect pheromone within an area (Moore's Neighbourhood);
- *State 2 - Next Position Decision*: the robots use a selection strategy to determine their next destination cell (Inertial strategy – refer to [Tinoco et al. 2020]);
- *State 3 - Pheromone Deposition*: the robots deposit pheromone in their local maps through Equation 1.

$$\Delta_{ij}^{k} = (\psi_{max} - \psi_{ij}^{s}) \cdot \left[\alpha \cdot (\delta \cdot e)^{\eta \cdot \frac{r}{\pi}}\right] \tag{1}$$

where:

Δ_{ij}^{k} : pheromone deposited by the robot $\{k\}$ in the cell $\{ij\}$;
ψ_{max} : max. pheromone concentration in a cell;
ψ_{ij}^{t} : pheromone concentration in the cell $\{ij\}$ at time-step $\{t\}$;
r : distance of the cell $\{ij\}$ from the robot r $\{r \in \mathbb{N} \mid 0 \leq r \leq r_d\}$;
e : exponential constant (2.718281);
α : maximum deposited pheromone $\{\alpha \in \mathbb{R} \mid 0.0 \leq \alpha \leq 1.0\}$;
δ : influence of the deposition rate; and,
η : compensation of the evaporation rate.

- *State 4 – Pheromone Evaporation*: at each time-step, robots evaporate pheromone in their local maps to support cyclical task execution. The updated pheromone concentration in each cell x_{ij} is computed using Eq. 2.

$$\psi_{ij}^{t+1} = \left[\psi_{ij}^{t} - (\beta \cdot \psi_{ij}^{t})\right] + \sum_{k=1}^{N} \Delta_{ij}^{k} \tag{2}$$

where:

ψ_{ij}^{t+1} : updated pheromone in cell $\{ij\}$ at time-step $\{t+1\}$;
ψ_{ij}^{t} : pheromone concentration in cell $\{ij\}$ at time-step $\{t\}$;
β : pheromone evaporation rate; and,
Δ_{ij}^{k} : pheromone deposited by robot $\{k\}$ in cell $\{ij\}$ (refer to Eq. 1).

- *State 5 - Movement*: represents the robot's transition from an origin cell c_{ij} to a target cell $c_{(i+a)(i+b)}$ in its neighbourhood, such that $\{a, b \in \mathbb{Z}\}$;
- *State 6 – Dissemination*: robots share local pheromone data with nearby peers. Messages contain the robot ID, time-step, and pheromone data (Eq. 3).

$$message : [id \frown \textit{time-step} \frown \{phero.\ data\}] \tag{3}$$

- *State 7 – Aggregation*: robots merge received pheromone data with their local maps, integrating only higher concentrations to reflect more recent information and filtering duplicates to maintain map accuracy; and,
- *State 8 - End*: is activated when the robot completes the proposed task or reaches a limit of T time-steps.

In PheroCom, robots exchange pheromone data with nearby peers within a transmission radius, forming temporary communication networks. Robots can aggregate received information and re-disseminate it to nearby robots, enabling information to propagate across the swarm without handshaking. This exchange supports decentralised coordination and contributes to the emergence of global behaviour during task execution.

2.3. Entropy

Entropy, known as Shannon entropy [Shannon 1948], is a measure of uncertainty or unpredictability in a dataset. The more diverse the data, the higher the entropy; the more repetitive the values, the lower the entropy. For example, consider the set $A = 2, 2, 2, 2, 2, 2, 2, 2, 2, 2$. In this case, all values are identical. When randomly selecting an element, the probability of obtaining the value 2 is 100%. Since there is no uncertainty, the entropy is equal to 0.0, i.e., completely predictable. Now, consider the set $B = 1, 2, 3, 4, 5, 6, 7, 8, 9, 10$, where all values are different and appear with the same frequency. When selecting a number, each value has the same probability (10%) of being chosen. In this scenario, it is not possible to predict which number will be selected, characterizing a higher entropy value, i.e., high unpredictability.

In this work, an adaptation of entropy is applied to the cell visitation frequencies recorded in the cellsteps map. Entropy is used as a quantitative measure of how uniformly the swarm explores the environment. More homogeneous visitation patterns tend to produce lower entropy values, whereas concentrated exploration in a limited number of cells results in higher values. Consequently, entropy provides an indirect measure of spatial coverage quality and can be incorporated into the optimization process to favour balanced exploration behaviours. Equation 4 defines the Shannon entropy calculation.

$$E(X) = -\sum_{i=1}^{n}(P(x_i) \times log_2(P(x_i))) \tag{4}$$

where:

$E(X)$: entropy of the dataset X;
n : number of distinct values in the dataset;
x_i : each distinct value in the dataset; and,
$P(x_i)$: probability of occurrence of x_i in the dataset.

2.4. Task-Points

Task-points represent the completion of a surveillance cycle, which occurs when all rooms in the environment are visited by at least one robot. Each task-point indicates that the swarm has fully covered the environment. This metric quantifies coverage efficiency by analysing how frequently all rooms are visited within a given time, as well as temporal consistency: long intervals between task-point completions may indicate anomalies, such as delays in movement and inefficiencies in room transitions.

Definition 1 *Let **A** be an environment composed of **m** rooms and **E** a swarm composed of **n** robots. A room i belonging to environment A is defined as $\{s_i \mid (i \leq m)$ and $(i \in \mathbb{N})\}$. Similarly, a robot i belonging to swarm E is defined as $\{rb_i \mid (i \leq n)$ and $(i \in \mathbb{N})\}$. Therefore, a task-point is achieved if and only if every room $s_i \in A$ is visited by at least one robot $rb_i \in E$.*

In this work, task-points represent the performance component of the evaluation process. While entropy measures the homogeneity of swarm dispersion, task-points quantify how efficiently the environment is repeatedly covered. Together, these metrics enable the assessment of both coverage quality and surveillance effectiveness.

3. Proposition

This work proposes using GA to automatically optimize the parameters of the PheroCom model [Tinoco et al. 2025]. An entropy-based *fitness* function was adapted to promote a more homogeneous swarm distribution and evaluate collective performance through coverage quality. Section 3.1 presents the GA modelling and its integration with PheroCom, while Section 3.2 introduces the proposed entropy metric.

3.1. Genetic Algorithm Modelling

The GA (Fig. 2) integrates with the PheroCom model by evaluating individuals through a *fitness* function based on an adapted entropy metric and task-points. Entropy measures spatial distribution, while task-points reflect task performance.

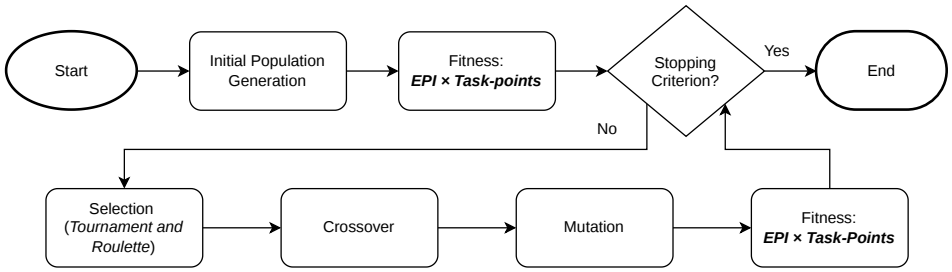


Figure 2. GA integrating the PheroCom model into the evaluation of individuals.

The initial population consists of individuals represented by vectors of seven real-valued parameters (Fig. 3): *evaporation*, *elitist*, *stochastic*, *inertial*, *alpha*, *delta*, and *eta*. These parameters control pheromone dynamics and robot decision-making.

PheroCom Model Parameters

[0]	[1]	[2]	[3]	[4]	[5]	[6]
0.72	0.56	0.84	0.29	0.63	0.45	0.91
Evaporation	Elitist	Stochastic	Inertial	Alpha	Delta	Eta

Figure 3. Example of a parameter vector for the PheroCom model.

Individuals evolve through selection (tournament and roulette), uniform crossover, and additive mutation. Elitism preserves the best solutions, and the process iterates for a predefined number of generations to discover improved configurations.

3.2. Fitness Function

The fitness function evaluates both task execution and spatial distribution. It is defined as:

$$F = E \times \mathcal{T} \tag{5}$$

where F is the fitness value, E is entropy, and τ is the number of achieved task-points.

Entropy reflects swarm dispersion and encourages more homogeneous coverage. Only free cells are considered, avoiding distortion from walls. This combination guides the GA toward solutions that balance performance and spatial distribution.

3.2.1. Entropy Based on Distinct Values

For the proposed application, Shannon entropy requires two mathematical adaptations: normalization and inversion of its interpretation. First, entropy is normalized to the interval $[0, 1]$ using Equation 6. Second, since the inverse of entropy represents homogeneity, Equation 7 is applied accordingly. However, Shannon entropy does not account for visitation magnitude, which represents an additional consideration addressed by the EPI metric in the following section.

$$E_{\text{norm}} = \frac{E_{\text{Sh}}}{\log_2(n)} \tag{6}$$

$$E_{\text{inv}} = 1.0 - E_{\text{norm}} \tag{7}$$

3.2.2. Entropy Proportional to Intensity

Entropy Proportional to Intensity (EPI) extends Shannon entropy by incorporating visitation magnitude. Let x_{ij} represent a cell at position (i, j). The final EPI formulation, considering only free cells, is given by Equation 11:

The Proportional Frequency (PF) of a cell x_{ij} is defined as:

$$PF_{ij} = \frac{FB_{ij}^{\gamma}}{\sum_{k=1}^{n}\sum_{l=1}^{m} FB_{kl}^{\gamma}} \tag{8}$$

Replacing relative to proportional frequency in Shannon entropy:

$$E_{int} = -\sum_{i=1}^{n}\sum_{j=1}^{m} (PF_{ij} \cdot \log_2(PF_{ij})) \tag{9}$$

Substituting Equation 8 into Equation 9:

$$E_{int} = -\sum_{i=1}^{n}\sum_{j=1}^{m} \left(\frac{FB_{ij}^{\gamma}}{\sum_{k=1}^{n}\sum_{l=1}^{m} FB_{kl}^{\gamma}} \cdot \log_2 \left(\frac{FB_{ij}^{\gamma}}{\sum_{k=1}^{n}\sum_{l=1}^{m} FB_{kl}^{\gamma}} \right) \right) \tag{10}$$

Applying normalization:

$$E_{int} = -\frac{1}{\log_2(n)} \sum_{i=1}^{n}\sum_{j=1}^{m} \left(\frac{FB_{ij}^{\gamma}}{\sum_{k=1}^{n}\sum_{l=1}^{m} FB_{kl}^{\gamma}} \cdot \log_2 \left(\frac{FB_{ij}^{\gamma}}{\sum_{k=1}^{n}\sum_{l=1}^{m} FB_{kl}^{\gamma}} \right) \right) \tag{11}$$

where:

E_{int} : resulting entropy value;
PF_{ij} : proportional visitation frequency;
FB_{ij} : raw visitation frequency;
γ : exponent used to amplify differences; and,
$n \times m$: total number of valid cells.

This formulation produces a continuous distribution based on visitation intensity, allowing a more accurate assessment of spatial balance than the Shannon entropy.

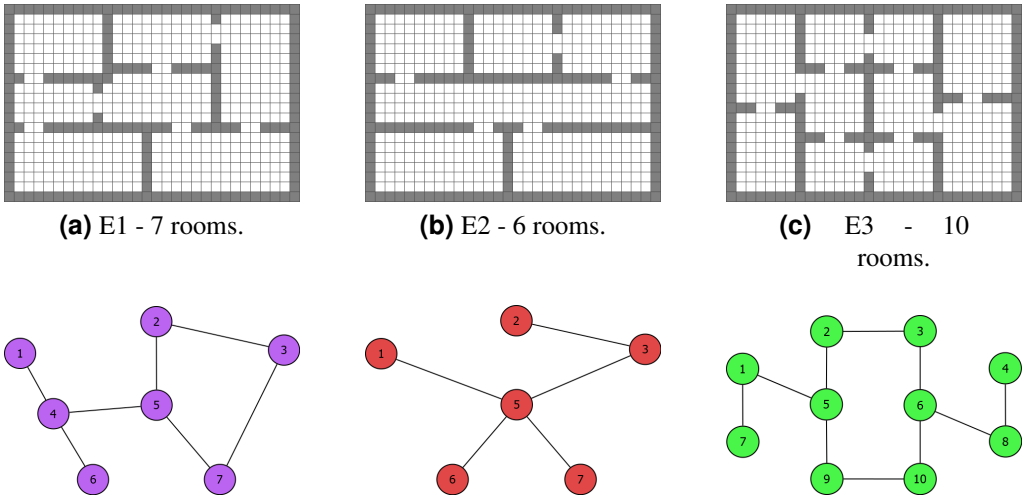
4. Experiments and Analysis

This Section presents the experiments and analyses conducted to optimize the parameters of the PheroCom [Tinoco et al. 2025] using GA. A *fitness* function based on entropy (see Section 3.2.2) was employed to promote homogeneous swarm dispersion. Section 4.1 describes the experimental setup, while Section 4.2 presents the results and discussion.

4.1. Experimental Setup

All experiments were executed using the MaSS platform. Due to the high computational demand of evolutionary optimization, a high-performance implementation was required. Overhead from graphical interfaces and physical force simulations was avoided.

Figure 4 shows the environments and their corresponding room connectivity graphs. The grids (Figs. 4a, 4b and 4c) represent indoor layouts composed of rooms connected by doors, while the graphs (Figs. 4d, 4e and 4f) provide an abstract representation of room connectivity, facilitating the identification of structural characteristics.



(a) E1 - 7 rooms. **(b)** E2 - 6 rooms. **(c)** E3 - 10 rooms.

(d) Graph of A1. **(e)** Graph of A2. **(f)** Graph of A3.

Figure 4. Representation of the simulation environments through regular grids (20×30 cells) and their corresponding room connectivity graphs.

Regarding GA parameters, population sizes of 50, 100, and 150 individuals were evaluated over 100 generations. Each individual was assessed through 30 executions of the PheroCom model[1], each consisting of 1000 time-steps and a swarm of three robots. As shown in Table 2, 12 configurations combining population sizes and mutation rates (2% to 8%) were evaluated to analyse their impact on convergence and performance.

Table 2. Configurations of mutation rate and population size tested in the GA.

Configurations	C1	C2	C3	C4	C5	C6	C7	C8	C9	C10	C11	C12
Mutation (%)	2	4	6	8	2	4	6	8	2	4	6	8
Population	50	50	50	50	100	100	100	100	150	150	150	150

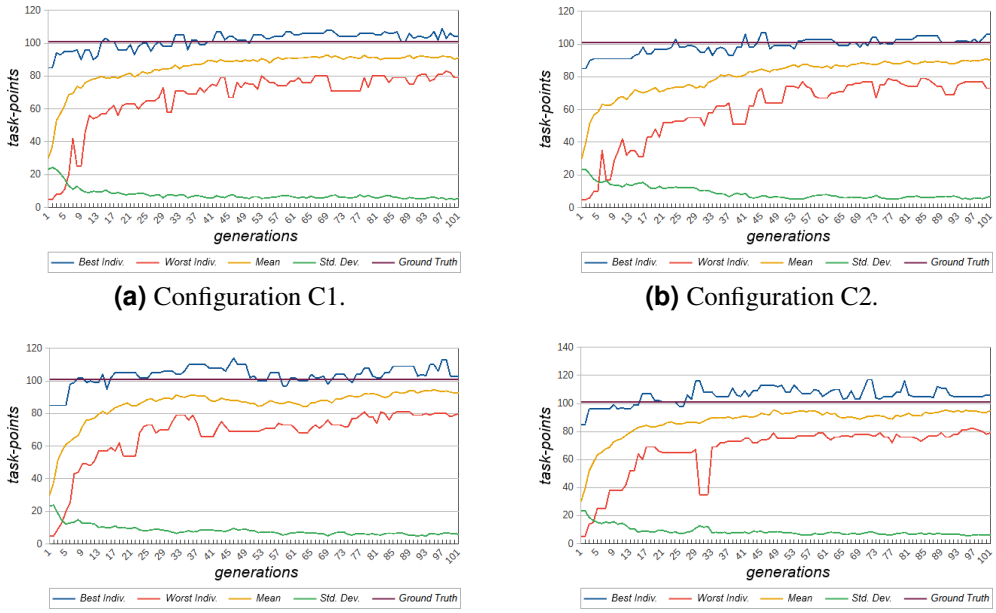
[1]Experiments were carried out on a 2x Intel Xeon E5-2680v4 CPUs @2.40–3.30GHz, 128GB RAM, AMD Radeon RX580 8GB GPU, running Fedora 44.

4.2. Experiments

This section presents the results for the evaluated configurations. The metrics include Best and Worst individuals, Mean, Standard Deviation, and Ground Truth. The ground truth is fixed at 101 task-points [Tinoco et al. 2020]. Each individual is evaluated based on the mean performance over 30 runs.

4.2.1. Exp-01: GA with population of 50 individuals

Figure 5 shows the results for configurations C1–C4. Configuration C4 (8% mutation) achieved the highest value, reaching 117 task-points. All configurations surpassed the ground truth. Despite entropy-based penalization, performance remained close to or above the reference, indicating nearly homogeneous coverage.



(a) Configuration C1. **(b)** Configuration C2.

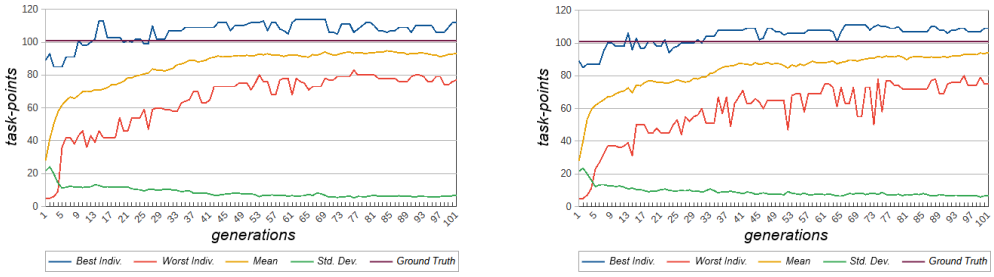
(c) Configuration C3. **(d)** Configuration C4.

Figure 5. Evolution across generations of the GA for configurations C1 to C4.

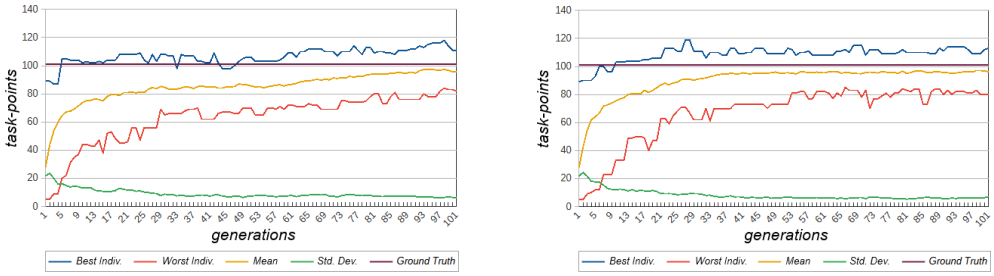
Population quality improved over generations. In C4, the mean reached 95.16 ± 5.86 at generation 94 ($\approx 5.8\%$ below the ground truth), reflecting effective elitism and genetic operators. The worst individuals mean 81.4% ($\approx 80.7\%$ of the ground truth), indicating consistent improvement across the population.

4.2.2. Exp-02: GA with population of 100 individuals

With 100 individuals (Fig. 6), all configurations (C5–C8) surpassed the ground truth. The best result (119 task-points) again occurred at 8% mutation (C8), only 3–5 points above the 50-individual case. Higher mutation rates introduced oscillations, balancing exploration and exploitation while preventing premature convergence.



(a) Configuration C5. **(b)** Configuration C6.

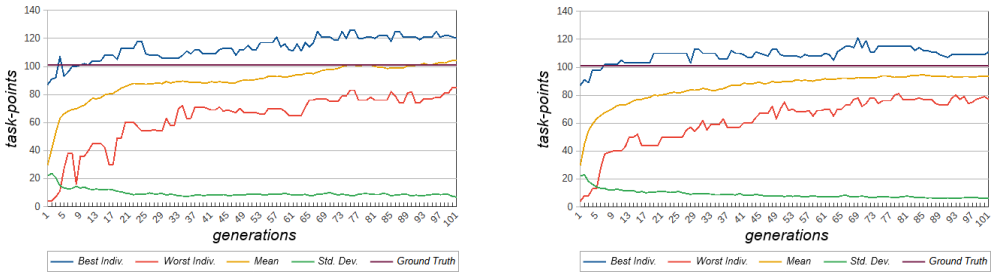


(c) Configuration C7. **(d)** Configuration C8.

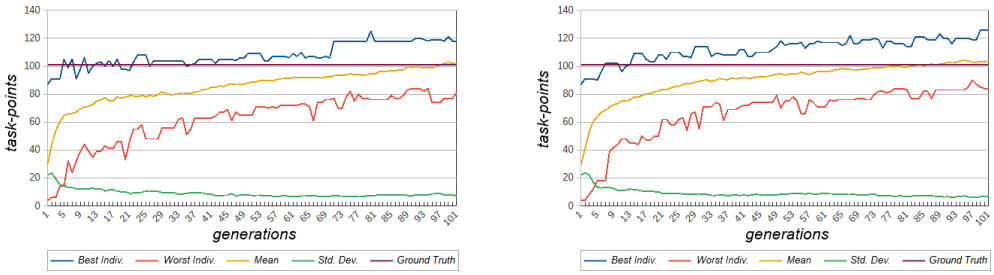
Figure 6. Evolution across generations of the GA for configurations C5 to C8.

4.2.3. Exp-03: GA with population of 150 individuals

With 150 individuals (Fig. 7), the largest improvements were observed: $\approx 24.4\%$ above the ground truth. C9 achieved the highest mean increase ($\approx 12.51\%$), followed by C12 ($\approx 9.47\%$). Both reached the highest value (126 task-points), with the 150-individual configurations consistently surpassing the ground truth by a substantial margin.



(a) Configuração C9. **(b)** Configuração C10.

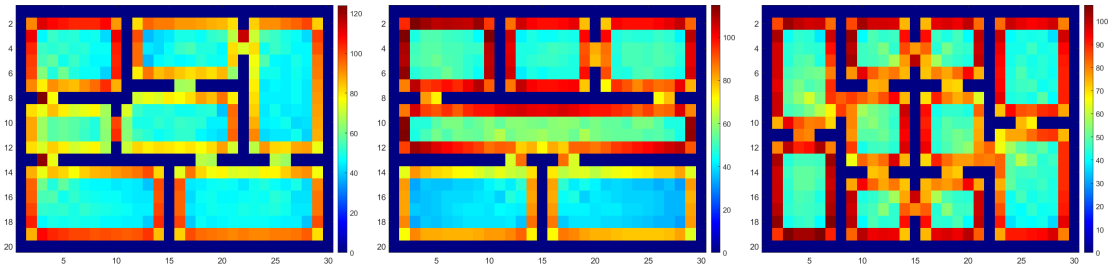


(c) Configuração C11. **(d)** Configuração C12.

Figure 7. Evolution across generations of the GA for configurations C9 to C12.

4.2.4. Exp-04: Cellsteps Maps

Cellsteps maps represent swarm dispersion over time. Figure 8 shows the best configuration. The distribution is mostly uniform (45 visits), with higher values in central rooms (65) due to graph connectivity and near walls (100) due to pheromone dynamics. Although coverage is adequate, some imbalance remains.



(a) E1 cellsteps map. **(b)** E2 cellsteps map. **(c)** E3 cellsteps map.

Figure 8. Swarm cellsteps dispersion maps using the best-evolved parameters.

5. Conclusion and Future Work

This work investigated the use of GA to automatically tune the PheroCom parameters [Tinoco et al. 2025], using entropy in the fitness function to promote balanced spatial coverage and improved swarm performance. The hypothesis was that entropy could measure exploration uniformity and guide the GA toward more efficient coverage. Entropy was adapted through EPI, which incorporates visitation magnitude, with two challenges: balancing sensitivity and robustness, and determining its influence on fitness.

The obtained results validate our hypothesis: the integration of entropy as an evaluation metric enabled an effective analysis of exploration homogeneity, favouring solutions with a more balanced distribution of robots across the environment and reducing the neglect of specific regions. In addition, the parameter optimization using GA consistently outperformed manual configuration, increasing the overall efficiency of the model by approximately 24.75%. However, it was also observed that entropy alone does not directly evaluate the temporal continuity of surveillance, which may limit its application in continuous monitoring tasks over extended periods.

Future works include: (i) incorporating additional complementary metrics alongside entropy; (ii) exploring parallelization techniques to further reduce overall simulation time; (iii) evaluating the optimized model in different environments with varied topologies; (iv) extending the method to other domains, such as UAV coordination in precision agriculture; (v) investigating alternative bio-inspired optimization approaches; and, (vi) optimizing coverage with respect to temporal homogeneity.

Acknowledgments

This work was supported by FAPEMIG, CNPq and CAPES.

Disclosure of Generative AI

The authors used Generative AI tools solely for language polishing and clarity improvement. The authors retain full responsibility for the content of this manuscript.

References

Cheng, K. P., Mohan, R. E., Nhan, N. H. K., and Le, A. V. (2020). Multi-objective genetic algorithm-based autonomous path planning for hinged-tetro reconfigurable tiling robot. *IEEE Access*, 8:121267–121284.

Halder, S. and Afsari, K. (2023). Robots in inspection and monitoring of buildings and infrastructure: A systematic review. *Applied Sciences*, 13(4):2304.

Hao, K., Zhao, J., Yu, K., Li, C., and Wang, C. (2020). Path planning of mobile robots based on a multi-population migration genetic algorithm. *Sensors*, 20(20):5873.

Huang, Y., Wu, S., Mu, Z., Long, X., Chu, S., and Zhao, G. (2020). A multi-agent reinforcement learning method for swarm robots in space collaborative exploration. In *Int. Conf. on Control, Auto. and Robotics (ICCAR)*, pages 139–144, Singapore. IEEE.

López-González, A., Campaña, J. M., Martínez, et al. (2020). Multi robot distance based formation using parallel genetic algorithm. *Applied Soft Comp.*, 86:105929.

Ma, J., Liu, Y., Zang, S., Wang, L., et al. (2020). Robot path planning based on genetic algorithm fused with continuous bezier optimization. *Comp. Intell. Neurosci.*, 2020.

Nonoyama, K. et al. (2022). Energy-efficient robot configuration and motion planning using genetic algorithm and particle swarm optimization. *Energies*, 15(6):2074.

Papazoglou, G. and Biskas, P. (2023). Review and comparison of GA and particle swarm optimization in the optimal power flow problem. *Ene.*, 16(3):1152.

Raj, R. and Kos, A. (2022). A comprehensive study of mobile robot: History, developments, applications, and future research perspectives. *Apl. Sci.*, 12(14):6951.

Şahin, E. (2004). Swarm robotics: From sources of inspiration to domains of application. In *Int. W. Swarm Robotics*, pages 10–20, Berlin, Alemanha. Springer.

Shahzad, M. M., Saeed, Z., Akhtar, A., Munawar, H., Yousaf, M. H., Baloach, N. K., and Hussain, F. (2023). A review of swarm robotics in a nutshell. *Drones*, 7(4):269.

Shannon, C. E. (1948). A mathematical theory of communication. *The Bell system technical journal*, 27(3):379–423.

Stolfi, D. H., Brust, M. R., Danoy, G., and Bouvry, P. (2020). A cooperative coevolutionary approach to maximise surveillance coverage of uav swarms. In *Annual Consumer Comm. & Netw. Conf. (CCNC)*, pages 1–6, Las Vegas, Estados Unidos. IEEE.

Tinoco, C. R., Martins, L. G. A., and Oliveira, G. M. (2025). PheroCom: Decentralised and asynchronous robot swarm coordination framework based on virtual pheromone and vibroacoustic communication. *Swarm and Evolutionary Computation*, 99:102083.

Tinoco, C. R., Vizzari, G., and Oliveira, G. M. B. (2020). Parameter adjustment of a bio-inspired coordination model for swarm robotics using evolutionary optimisation. In *Int. Conf. Cell. Aut. Res. Ind. (ACRI)*, pages 146–155, Łódź, Poland. Springer.

Torres, G. A. S., Calumba, S. P., Fajardo, F., et al. (2024). Genetic algorithm-driven optimization for enhanced accessibility in mobile robotics. In *Int. Conf. Ctrl. Auto. Rob. (ICCAR)*, pages 109–115, Orchard District, Singapore. IEEE.

Zhan, Z.-H., Shi, L., Tan, K. C., and Zhang, J. (2022). A survey on evolutionary computation for complex continuous optimization. *Artificial Intell. Review*, 55(1):59–110.